

Nonlocal theory of collective excitations in quantum-dot arrays

Weiming Que, George Kirczenow, and Eleuterio Castaño

Department of Physics, Simon Fraser University, Burnaby, British Columbia, Canada V5A 1S6

(Received 25 June 1990; revised manuscript received 30 January 1991)

We present a nonlocal theory of collective excitations in quantum-dot arrays. Selection rules, oscillator strengths, and Coulomb interactions inside a dot and between dots are discussed. The collective excitation energy is found to "saturate" for n_0 (the number of electrons per dot) greater than 3. The depolarization energy shift in a quantum-dot array is found to be predominantly due to interdot coupling. We explain qualitatively the multiple branches and anticrossings recently observed in far-infrared experiments. We predict that anticrossings can occur only if $n_0 > 2$. If $n_0 \leq 2$, there should be only one branch with positive B dispersion, and one branch with negative B dispersion, where B represents a perpendicular magnetic field. Multiple branches with positive (negative) B dispersions occur for larger n_0 . The use of left (right) -circularly-polarized light should result in signals predominantly from positive (negative) B dispersion branches, while signals from the opposite polarization branches should provide information on the coupling between positive and negative B dispersion branches.

I. INTRODUCTION

Quantum dots are structures that confine electrons in all three spatial dimensions. They are typically a few hundred nanometers long or wide and a few nanometers thick. In such small structures electron states are quantized into discrete energy levels, with energy spacings between levels ranging from a few meV to ten times more.¹ Contrary to what one might think, quantum-dot systems are far from simple. Experiments on them have revealed numerous surprises. An example is the recent discovery of multiple branches of excitations and anticrossings between branches in far-infrared (FIR) experiments on quantum-dot systems in a magnetic field.² These surprising results have provided incentives for theorists to seek a thorough understanding of these phenomena.

The capability of fabricating quantum dots is fairly recent, but it has already created a dynamic field of study. Experiments on quantum-dot systems can be roughly grouped into two categories: transport experiments and optical experiments. In transport experiments, it is possible to study a single quantum dot, or a few quantum dots in various configurations. In optical (FIR) experiments, macroscopic samples are used in order to obtain detectable signal strength. A typical sample several millimeters long and wide can contain tens of millions of quantum dots. Due to the presence of the long-range Coulomb force, in such systems the quantum dots are Coulomb coupled, making these systems exhibit richer properties than isolated quantum dots. A single quantum dot containing only one electron can only have single-particle excitations, but an array of such dots can also support collective modes. The existence of collective excitations in such systems was predicted by Que and Kirczenow³ in 1988, before any optical (FIR) experiments on quantum-dot systems were attempted. Since then several FIR ex-

periments on quantum-dot systems have been carried out.^{2,4-6} Although quantitative comparisons to some of the key results are yet to be made, qualitatively the results are in agreement with the collective excitation picture, as we will show in this paper.

Reference 3 developed the basic formalism for the theoretical study of collective excitations in quantum-dot arrays. It considered a rectangular lattice of quantum dots in the absence of magnetic field. It showed that collective excitations should exist in quantum-dot systems, with energies shifted significantly from single-particle excitation energies. It also showed that a system with a dispersionless single-particle energy spectrum can have a dispersive collective energy spectrum, and that a degeneracy in the single-particle spectrum can be lifted in the collective spectrum. In this paper we extend this work to more general two-dimensional (2D) lattices of quantum dots, and include the effects of a magnetic field B . A magnetic field applied in the z direction couples the x and y degrees of freedom, changing the single-particle energy spectrum as well as the collective excitation spectrum. As we will show, many interesting effects occur in a magnetic field. Reference 3 is a special case of the more general theory presented in this paper. It can be recovered by taking $B = 0$.

In Sec. II we establish the general formalism. Section III is devoted to model calculations, assuming parabolic confinement. The parabolic confinement model has been used by many experimentalists to analyze their data. We will discuss selection rules, multiple branches, anticrossings, effects of level crossings in single-particle energy spectra, and the Coulomb interaction between dots versus inside dots. Many of the qualitative results are not limited to the parabolic confinement model. Section IV discusses the nonlocal aspect of the theory. Section V discusses oscillator strengths for optical excitations. Concluding remarks are presented in Sec. VI.

II. FORMALISM

We consider a system of quantum dots which form a two dimensional lattice. A magnetic field \mathbf{B} is applied perpendicular to the 2D plane. Since the quantum dots made today are much more confined in the vertical z direction than in the lateral directions, we only need to consider the lowest-energy level in the z direction. For many systems that have been studied, the individual quantum dots are physically separated, allowing little possibility for electrons to tunnel between dots. For such systems we can use the tight-binding ansatz,⁷

$$|\mathbf{k}, \alpha\rangle = \xi_z \sum_{\mathbf{r}_j} e^{i\mathbf{k}\cdot\mathbf{r}_j} \psi_\alpha(\mathbf{r}-\mathbf{r}_j) e^{-i(e/\hbar)\mathbf{A}\cdot\mathbf{r}_j}, \quad (2.1)$$

where ξ_z is the wave function for the lowest-energy level in the z direction, \mathbf{k} is a 2D wave vector, \mathbf{r} is a 2D vector, \mathbf{r}_j is a 2D lattice vector, ψ_α is the xy component of the wave function for a single quantum dot, α is a composite quantum number, and \mathbf{A} is the vector potential for the magnetic field.

Collective excitations are studied using the self-consistent-field formalism of Ehrenreich and Cohen.⁸ Starting from the integral form of the Poisson equation, we take Fourier transforms in x and y directions and get

$$V(\mathbf{q}, z) = \frac{2\pi e^2}{\epsilon q} \int dz' e^{-q|z-z'|} n(\mathbf{q}, z'), \quad (2.2)$$

where \mathbf{q} is a 2D wave vector, $q = |\mathbf{q}|$, and ϵ is the background dielectric constant ϵ_b multiplied by $4\pi\epsilon_0$. The

density response of the system to a Coulomb perturbation is given by

$$n(\mathbf{q}, z) = 2|\xi_z|^2 \sum_{a, a'} \langle a | V(\mathbf{r}, z) | a' \rangle \langle a' | e^{i\mathbf{q}\cdot\mathbf{r}} | a \rangle \times \frac{f_{a'} - f_a}{E_{a'} - E_a + \hbar\omega}, \quad (2.3)$$

where a is a composite quantum number, and f_a is the Fermi distribution function. Combining (2.2) and (2.3) and integrating out the z degree of freedom gives

$$V(\mathbf{q}) = \frac{4\pi e^2}{\epsilon q} I(q) \sum_{a, a'} \langle a | V(\mathbf{r}, z) | a' \rangle \langle a' | e^{i\mathbf{q}\cdot\mathbf{r}} | a \rangle \times \frac{f_{a'} - f_a}{E_{a'} - E_a + \hbar\omega}, \quad (2.4)$$

where $V(\mathbf{q}) = \int dz V(\mathbf{q}, z) |\xi_z|^2 |\xi_{z'}|^2$, and

$$I(q) = \int dz \int dz' e^{-q|z-z'|} |\xi_z|^2 |\xi_{z'}|^2. \quad (2.5)$$

Since $\langle a | V(\mathbf{r}, z) | a' \rangle = \sum_{\mathbf{q}'} V(\mathbf{q}') \langle a | e^{-i\mathbf{q}'\cdot\mathbf{r}} | a' \rangle$, (2.4) can be written as

$$V(\mathbf{q}) = \frac{4\pi e^2}{\epsilon q} I(q) \sum_{a, a', \mathbf{q}'} V(\mathbf{q}') \langle a | e^{-i\mathbf{q}'\cdot\mathbf{r}} | a' \rangle \langle a' | e^{i\mathbf{q}\cdot\mathbf{r}} | a \rangle \times \frac{f_{a'} - f_a}{E_{a'} - E_a + \hbar\omega}. \quad (2.6)$$

Using Eq. (2.1) we find

$$\langle a' | e^{i\mathbf{q}\cdot\mathbf{r}} | a \rangle = \sum_{\mathbf{r}_j, \mathbf{r}_{j'}} e^{i\mathbf{k}\cdot\mathbf{r}_j - i\mathbf{k}'\cdot\mathbf{r}_{j'}} \int dx \int dy e^{i(e/\hbar)(\mathbf{A}\cdot\mathbf{r}_{j'} - \mathbf{A}\cdot\mathbf{r}_j) + i\mathbf{q}\cdot\mathbf{r}} \psi_{\alpha'}^*(\mathbf{r}-\mathbf{r}_{j'}) \psi_\alpha(\mathbf{r}-\mathbf{r}_j). \quad (2.7)$$

In (2.7) we have direct terms when $\mathbf{r}_j = \mathbf{r}_{j'}$, and overlap terms when $\mathbf{r}_j \neq \mathbf{r}_{j'}$. For systems with no tunneling between quantum dots, such as those studied in the FIR experiments of Ref. 2, the overlap terms vanish. For such systems we get

$$\langle a' | e^{i\mathbf{q}\cdot\mathbf{r}} | a \rangle = \delta_{\mathbf{k}' - \mathbf{k} - \mathbf{q}, \mathbf{G}} A_{\alpha\alpha'}(\mathbf{q}), \quad (2.8)$$

$$A_{\alpha\alpha'}(\mathbf{q}) = \int dx \int dy e^{i\mathbf{q}\cdot\mathbf{r}} \psi_{\alpha'}^*(\mathbf{r}) \psi_\alpha(\mathbf{r}). \quad (2.9)$$

The neglect of overlap terms might be still valid for systems with weak tunneling.⁹ The δ function in (2.8) indicates that the wave vector is conserved within a reciprocal lattice vector \mathbf{G} due to the periodicity of the system. With (2.8) and (2.9), Eq. (2.6) becomes

$$V(\mathbf{q}) = \frac{4\pi e^2}{\epsilon q} I(q) \sum_{\mathbf{G}} V(\mathbf{q} + \mathbf{G}) \sum_{\alpha, \beta} A_{\alpha\beta}^*(\mathbf{q} + \mathbf{G}) A_{\alpha\beta}(\mathbf{q}) \times \sum_{\mathbf{k}} \frac{f_{a'} - f_a}{E_{a'} - E_a + \hbar\omega}. \quad (2.10)$$

It is understood that the quantum number $a' = (\mathbf{k} + \mathbf{q}, \beta)$. It is convenient to define

$$\Pi_{\alpha\beta}(\mathbf{q}, \omega) = \sum_{\mathbf{k}} \frac{f_{a'} - f_a}{E_{a'} - E_a + \hbar\omega}. \quad (2.11)$$

Note that if there is no tunneling between quantum dots, $\Pi_{\alpha\beta}$ becomes independent of \mathbf{q} .

To solve (2.10), we define

$$G_{\alpha\beta}(\mathbf{q}) = \sum_{\mathbf{G}} V(\mathbf{q} + \mathbf{G}) A_{\alpha\beta}^*(\mathbf{q} + \mathbf{G}). \quad (2.12)$$

$G_{\alpha\beta}(\mathbf{q})$ is periodic, $G_{\alpha\beta}(\mathbf{q}+\mathbf{G})=G_{\alpha\beta}(\mathbf{q})$. So is $\Pi_{\alpha\beta}(\mathbf{q},\omega)$. Using (2.12), replacing \mathbf{q} by $\mathbf{q}+\mathbf{G}$ in (2.10) gives

$$V(\mathbf{q}+\mathbf{G})=\frac{4\pi e^2}{\epsilon|\mathbf{q}+\mathbf{G}|}I(|\mathbf{q}+\mathbf{G}|) \times \sum_{\alpha,\beta} G_{\alpha\beta}(\mathbf{q}) A_{\alpha\beta}(\mathbf{q}+\mathbf{G}) \Pi_{\alpha\beta}(\mathbf{q},\omega). \quad (2.13)$$

Now we multiply (2.13) by $A_{\alpha'\beta'}^*(\mathbf{q}+\mathbf{G})$ and then sum over \mathbf{G} . The result is a set of homogeneous linear equations for $G_{\alpha\beta}(\mathbf{q})$:

$$G_{\alpha'\beta'}(\mathbf{q})=\sum_{\alpha,\beta} G_{\alpha\beta}(\mathbf{q}) \sum_{\mathbf{G}} \frac{4\pi e^2}{\epsilon|\mathbf{q}+\mathbf{G}|} I(|\mathbf{q}+\mathbf{G}|) A_{\alpha'\beta'}^*(\mathbf{q}+\mathbf{G}) \times A_{\alpha\beta}(\mathbf{q}+\mathbf{G}) \Pi_{\alpha\beta}(\mathbf{q},\omega). \quad (2.14)$$

In (2.14) α and β appear in pairs, describing transitions from the α th level to the β th level. From the definition of A in (2.9), it is obvious that the order of α and β cannot be interchanged unless wave functions of the system are real. Let us use i to denote the $\alpha\beta$ pair, and j to denote the $\alpha'\beta'$ pair. With this notation (2.14) appears less complicated,

$$G_j(\mathbf{q})=\sum_i G_i(\mathbf{q}) \Pi_i(\mathbf{q},\omega) \sum_{\mathbf{G}} \frac{4\pi e^2}{\epsilon|\mathbf{q}+\mathbf{G}|} I(|\mathbf{q}+\mathbf{G}|) \times A_j^*(\mathbf{q}+\mathbf{G}) A_i(\mathbf{q}+\mathbf{G}). \quad (2.15)$$

The coefficients of $G_i(\mathbf{q})$ in (2.15) form a matrix with elements

$$C_{ij}=\Pi_i(\mathbf{q},\omega) \sum_{\mathbf{G}} \frac{4\pi e^2}{\epsilon|\mathbf{q}+\mathbf{G}|} I(|\mathbf{q}+\mathbf{G}|) A_j^*(\mathbf{q}+\mathbf{G}) \times A_i(\mathbf{q}+\mathbf{G}) - \delta_{ij}. \quad (2.16)$$

C_{ij} is neither a symmetric nor a Hermitian matrix. In order for (2.15) to have nontrivial solutions, namely, for the system to sustain self-supporting eigenmodes, the frequency ω must be such that the determinant of the matrix (2.16) vanishes. This condition determines the excitation energies of collective modes in the system.

Our method for deriving Eq. (2.14) has been used before in the study of plasmons in multilayer semiconductor superlattices.⁹ Reference 9 showed that it is equivalent to a different method by Das Sarma and Quinn,¹⁰ because the two methods produced identical results. Our method has also been applied to quantum-wire superlattices.¹¹ The resultant equation is identical to the equation derived by Li and Das Sarma using a different method.¹²

The general formalism in this section applies to any 2D lattice of nontunneling quantum dots, with or without a magnetic field, at zero or finite temperatures. Collective excitation energies can be calculated provided that single-particle energy levels and wave functions are known.

III. PARABOLIC CONFINEMENT

So far we have not specified any details of individual quantum dots. Self-consistent numerical results for a

particular sample¹³ show that even if the defining cap layer is square shaped, the confining potential seen by electrons in a quantum dot has nearly circular symmetry. The energy levels are found to be insensitive to the charge in the dot at a fixed gate voltage, and the evolution of energy levels with increasing magnetic field is similar to that for a parabolic potential. These results make the parabolic confining potential model very appealing. In the presence of a magnetic field, this model potential offers exact analytic information on the single-particle energy states. The parabolic confining potential model has been widely used by experimentalists for interpreting their data. We devote this section to study this model.

We assume that the confining potential in a single quantum dot is parabolic: $U(\mathbf{r})=\frac{1}{2}m^*\omega_0^2r^2$, where m^* is the effective mass. In the presence of a magnetic field in the z direction, the single-particle Hamiltonian is

$$H=\frac{1}{2m^*}(\mathbf{P}+e\mathbf{A})^2+U(\mathbf{r}). \quad (3.1)$$

In the symmetric gauge $\mathbf{A}=(-\frac{1}{2}By,\frac{1}{2}Bx)$. The energy levels of this Hamiltonian are given by¹⁴

$$E_{nm}=(2n+|m|+1)\hbar\Omega+\frac{m}{2}\hbar\omega_c, \quad (3.2)$$

where $\Omega=(\omega_0^2+\frac{1}{4}\omega_c^2)^{1/2}$, ω_c is the cyclotron frequency, m is the angular quantum number, $m=0,\pm 1,\pm 2,\dots$, and n is the radial quantum number, $n=0,1,2,\dots$. The wave functions are given by

$$\psi_{nm}=\frac{1}{\sqrt{2\pi}}e^{im\varphi}\left[\frac{2m^*\Omega n!}{\hbar(|m|+n)!}\right]^{1/2}\rho^m L_n^{|m|}(\rho^2)e^{-\rho^2/2}, \quad (3.3)$$

where $\rho=r(m^*\Omega/\hbar)^{1/2}$, and $L_n^{|m|}$ are associated Laguerre polynomials.

Figure 1 shows the energy spectrum (3.2). At high magnetic fields, magnetic confinement dominates over static confinement, and electron states group into quasidegenerate Landau levels. At zero magnetic field, static confinement determines the level structure to be that of a 2D harmonic oscillator. In between the two limits, energy level crossings appear. Note that if $\omega_0=0$, the energy levels would be simply Landau levels and no level crossings would occur. Therefore the level crossings are a quantum confinement effect.

A. Selection rules

The energy spectrum in Fig. 1 looks complicated. If there were no selection rules, there could be many possible excitations between levels. However, selection rules greatly narrow down the possible kinds of excitations. In optical experiments, the leading component in the outgoing signal usually comes from the dipole term $\langle a'|\mathbf{r}|a\rangle$. Selection rules are determined by conditions under which the matrix element $\langle a'|\mathbf{r}|a\rangle$ does not vanish. Using the tight-binding approximation (2.1) for a quantum-dot array, and neglecting overlap terms we get

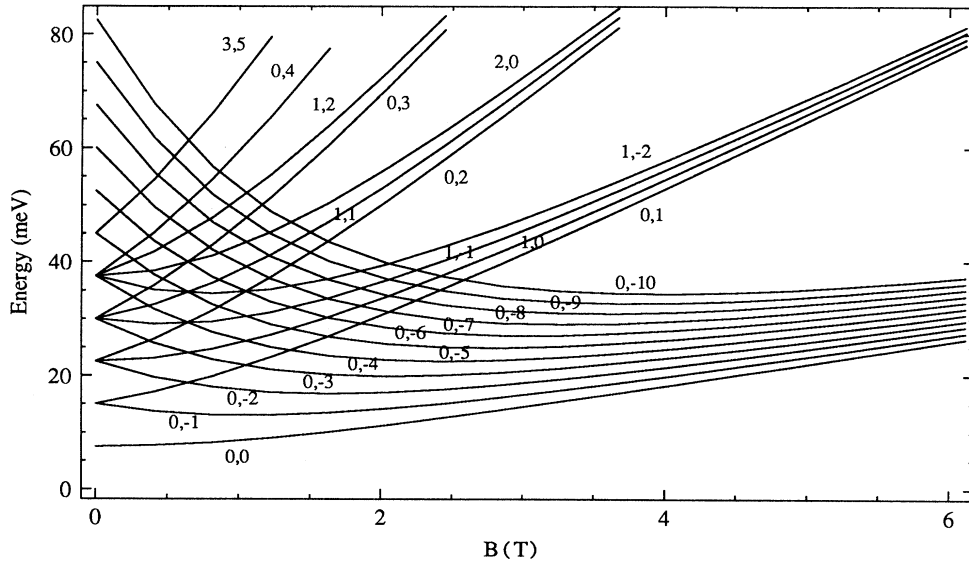


FIG. 1. Magnetic field dependence of the energy levels described by (3.2). The levels are labeled by (n, m) values. Confinement energy $\hbar\omega_0 = 7.5$ meV, $m^* = 0.014m_e$.

$$\langle a' | \mathbf{r} | a \rangle = \delta_{\mathbf{k}' - \mathbf{k}, \mathbf{G}} \int dx \int dy \psi_{\alpha'}^*(\mathbf{r}) \mathbf{r} \psi_{\alpha}(\mathbf{r}). \quad (3.4)$$

The integral in (3.4) is the matrix element for a single quantum dot, $\langle \alpha' | \mathbf{r} | \alpha \rangle$. Thus for quantum-dot arrays with negligible tunneling, the selection rules are the same as those for a single quantum dot. Any violation is only

of the order of the overlap integral between nearest-neighbor quantum dots. A similar conclusion should also apply to quantum-wire arrays.^{15,11}

Since the magnetic field couples the x and y degrees of freedom, it is better to consider $\langle \alpha' | x \pm iy | \alpha \rangle$ instead of $\langle \alpha' | x | \alpha \rangle$ and $\langle \alpha' | y | \alpha \rangle$ separately. Using the wave functions (3.3), we find

$$\begin{aligned} \langle n' m' | x \pm iy | n m \rangle = & \left[\frac{\hbar}{m^* \Omega} \right]^{1/2} \delta_{m', m \pm 1} \left[\left[n + m + \frac{1 \pm \text{sgn}(m)}{2} \right]^{1/2} \delta_{n', n} \right. \\ & \left. - \left[n + \frac{1 \mp \text{sgn}(m)}{2} \right]^{1/2} \delta_{n', n \mp \text{sgn}(m)} \right], \quad m \neq 0, \end{aligned} \quad (3.5)$$

and

$$\begin{aligned} \langle n' m' | x \pm iy | n m \rangle = & \left[\frac{\hbar}{m^* \Omega} \right]^{1/2} \delta_{m', \pm 1} \\ & \times (\sqrt{n+1} \delta_{n', n} - \sqrt{n} \delta_{n', n-1}), \\ & m = 0. \end{aligned} \quad (3.6)$$

The δ functions in (3.5) and (3.6) give the selection rules $\Delta n = 0, \pm 1$, and $\Delta m = \pm 1$. Namely, the radial quantum number n cannot change by more than one, and the angular number m can only change by one. The single-particle energy for transitions obeying the selection rules can take only two values:

$$\Delta E_{\pm} = \hbar\Omega + \frac{\Delta m}{2} \hbar\omega_c = \hbar(\omega_0^2 + \frac{1}{4}\omega_c^2)^{1/2} \pm \frac{1}{2} \hbar\omega_c, \quad (3.7)$$

where the $+$ ($-$) sign corresponds to left (right) circular polarization.

The selection rules and (3.7) have very important consequences. In a somewhat simplistic picture, collective excitations in quantum dots may be understood as a result of Coulomb coupling between single-particle excitations, with energies given by the single-particle energies (3.7) plus a “depolarization shift” due to Coulomb coupling. The magnetic field dependence of the collective excitation energy is largely influenced by ΔE_{\pm} . Note that ΔE_{+} increases with magnetic field B , approaching $\hbar\omega_c$ in the high field limit, while ΔE_{-} decreases with B . De-

pending on where the Fermi level is or how many electrons each quantum dot contains, the system can have many selection-rule-obeying single-particle excitations with different initial and final states, but they are largely degenerate, having only two distinct energies ΔE_{\pm} . However, the matrix elements for Coulomb interaction $\langle a|V|a' \rangle$ are generally different for different $|a \rangle$ and $|a' \rangle$, causing the degeneracy to be broken in the collective energy spectrum. This means that, in the parabolic confinement model, while single-particle excitations have only one positive B dispersion branch ΔE_{+} and one negative B dispersion branch ΔE_{-} , collective excitations can have multiple branches of each type. Indeed multiple branches have been observed experimentally.² The existence of multiple branches is more obvious if the confinement is nonparabolic. In that case one finds that multiple branches already exist in the single-particle spectrum. Clearly the existence of multiple branches originates from the fact that there can be several excitations obeying the selection rules. Therefore in essence it is not a collective phenomenon.

Since optical (FIR) wavelengths are orders of magnitude larger than typical quantum-dot sizes, the dipole selection rules govern the optical excitations very precisely. Therefore for theoretical calculations it is not necessary to consider excitations forbidden by the dipole selection rules. This statement may not apply to systems with tunneling, in which the selection rules for a single dot can be violated due to large wave-function overlaps between quantum dots.

B. Model calculations

For parabolic confinement in x and y directions, the quantity $A_{\alpha\beta}(\mathbf{q})$ can be calculated straightforwardly using the definition (2.9) and wave functions (3.3). Making use of the expansion

$$e^{ix \cos \varphi} = \sum_{n=-\infty}^{\infty} i^n J_n(x) e^{in\varphi}, \quad (3.8)$$

where J_n are Bessel functions of the first kind, we find that for $\alpha=(n, m)$ and $\beta=(n', m')$,

$$A_{\alpha\beta}(\mathbf{q}) = 2e^{i(m-m')\varphi_0} \left[\frac{n!n'}{(|m|+n)!(|m'|+n')!} \right]^{1/2} (-i)^{m'-m} \\ \times \int_0^{\infty} d\rho \rho^{|m|+|m'|+1} L_n^{|m|}(\rho^2) L_{n'}^{|m'|}(\rho^2) e^{-\rho^2} J_{m-m'}(\rho q (\hbar/m^* \Omega)^{1/2}), \quad (3.9)$$

where $\varphi_0 = \arctan(q_y/q_x)$, provided $q \neq 0$. If $q = 0$, $A_{\alpha\beta}$ is simply the orthonormal product $\langle \beta | \alpha \rangle$, giving zero or one depending on whether α is different from β or not.

The confinement in the z direction can be achieved by sandwiching materials.¹⁶ For such quantum dots the z degree of freedom can be described by "particle in a box" wave functions, and we can use

$$\xi_z = \left[\frac{2}{z_0} \right]^{1/2} \sin \left[\frac{\pi z}{z_0} \right] \quad (3.10)$$

for the z component wave function, with z_0 the thickness of the layer in which electrons are confined. This wave function and the definition of $I(q)$ in (2.5) gives

$$I(q) = \frac{2}{qz_0} \left[1 + \frac{(qz_0)^2}{2[4\pi^2 + (qz_0)^2]} \right. \\ \left. - \frac{(2\pi)^4 (1 - e^{-qz_0})}{qz_0 [4\pi^2 + (qz_0)^2]^2} \right]. \quad (3.11)$$

In our calculations spin splitting is neglected, since we are interested in relatively low magnetic fields where spin splitting is not significant. We leave the effects of spin splitting at higher magnetic fields to future research.

The size of the matrix equation given by (2.14) is given by the number of interlevel transitions under consideration. Although we are only interested in excitations allowed by the dipole selection rules because they are the experimentally observable ones, in principle they can couple to excitations characterized by higher-order selection rules. This means that the corresponding off-diagonal matrix elements are nonzero, and our matrix equation has a dimension approaching infinity in the parabolic confinement model. In multilayer semiconductor superlattices, the "diagonal approximation," which replaces all off-diagonal matrix elements by zeros, has been used and is known to be a valid approximation if only the lowest subband is occupied.¹⁷ Recently, Que analyzed collective excitations in quantum-wire superlattices, and found that collective excitations characterized by different symmetries have very small off-diagonal matrix elements because of a cancellation effect.¹⁸ We expect the same cancellation effect to be present in a quantum-dot array, because it is a symmetry effect unrelated to the dimensionality of the system. In light of these results, in our calculations we restricted our matrix equation to be in the subspace of excitations allowed by the dipole selection rules. Within this subspace the matrix is treated exactly.

C. Multiple branches and anticrossings

When only the lowest-energy level is occupied, the selection rules of (3.6) allow only two excitations, from the state $(0,0)$ to $(0,-1)$, and from $(0,0)$ to $(0,1)$. Figure 2 shows the B dispersions of collective modes associated with these two transitions. The collective spectrum has one positive B dispersion branch, associated with the $(0,0) \rightarrow (0,1)$ transition, and one negative B dispersion branch, associated with the $(0,0) \rightarrow (0,-1)$ transition. At high magnetic fields there is a large energy splitting between the two branches. As B decreases, the positive and negative B dispersion branches approach each other. However, in the limit $B=0$, these modes do not have the same energy, a result of degeneracy breaking by Coulomb interaction. It has been shown that in the $B=0$ limit the two modes reduce to usual longitudinal and transverse modes.³ In Fig. 2 the energy difference between the two modes at $B=0$ is 0.09 meV. This small difference is difficult to measure experimentally. However, when the number of electrons per dot is increased to $n_0=4$ as in Fig. 3, the splitting between the top two modes at $B=0$ is 0.4 meV. This might be a measurable effect.

The number of allowed excitations increases with the number of occupied energy levels. We see from the above that if only the lowest-energy level is occupied, there are two allowed transitions. If $n_0=3$, one more level is occupied, we have the additional excitations $(0,-1) \rightarrow (0,-2)$, and $(0,-1) \rightarrow (1,0)$, making a

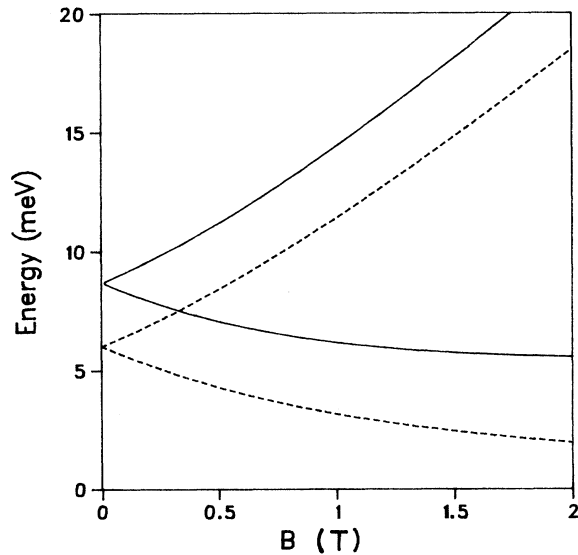


FIG. 2. B dispersions of collective excitation energies for two electrons per dot, $n_0=2$. The dashed lines show the single-particle excitation energies in Eq. (3.7). The system is a square lattice of quantum dots with lattice constant $d=250$ nm. Other parameters used are $\hbar\omega_0=6$ meV, $m^*=0.014m_e$, background dielectric constant $\epsilon_b=17$, $z_0=5$ nm, $q_x=q_y=0$, temperature $T=0$ K. The parameters are chosen to correspond to the InSb sample in Ref. 4.

total of four allowed excitations. With the breaking of degeneracy in the collective spectrum, we obtain multiple branches of collective modes as shown in Fig. 3(a). There are two positive B dispersion branches; the higher-energy branch has larger energy shifts from single-particle excitation energies, and is expected to have larger oscillator strengths.¹¹ There are also two negative B dispersion branches.

In Fig. 3(a) two of the branches seem to cross. Indeed they do cross if the two modes are uncoupled. In general coupling between branches is known to cause anticrossings. Deviations of the confining potential from azimu-

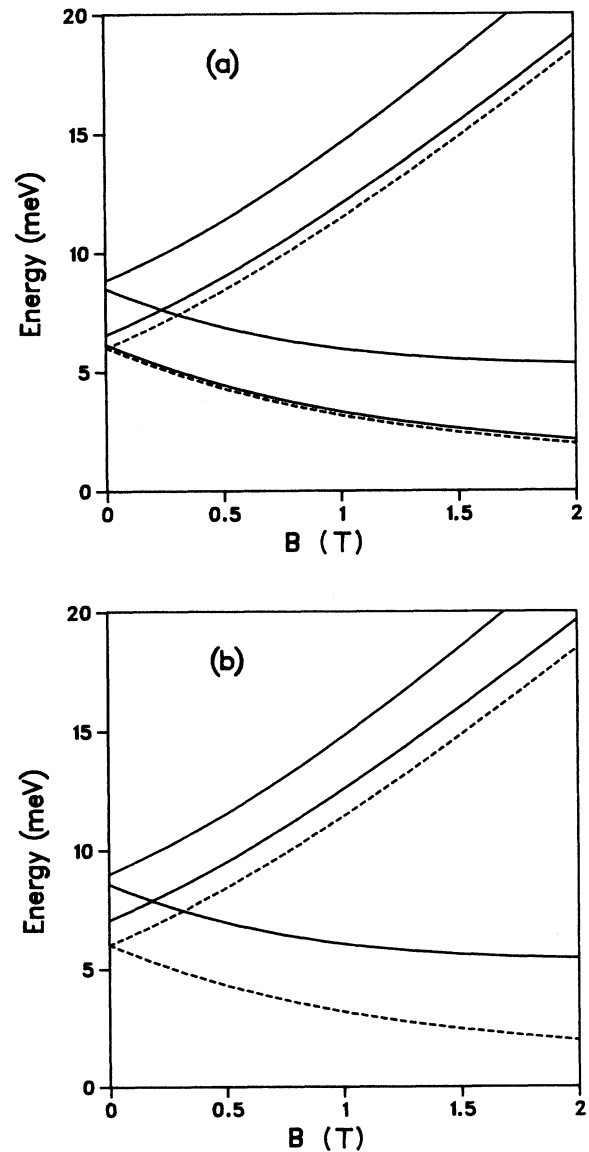


FIG. 3. B dispersions of collective excitation energies for (a) $n_0=3$; (b) $n_0=4$. The dashed lines show single-particle excitation energies in Eq. (3.7). Other parameters are the same as in Fig. 2.

thal symmetry or the parabolic shape can be expected to induce coupling between branches.

For $n_0=4$ and zero temperature, the $(0,0)\rightarrow(0,-1)$ transition is no longer possible because both states are fully occupied, making only three excitations possible. This is why in Fig. 3(b) there are only three branches. However, at finite temperatures the $(0,0)\rightarrow(0,-1)$ transition should be allowed due to partial occupation of the states, recovering the lowest-energy branch in Fig. 3(a). This suggests that experimental studies of the temperature dependence could be interesting.

Early experiments observed only one positive B dispersion branch, and some indications of a negative B dispersion branch.⁴ Recently, the much more accurate FIR experiments by Demel *et al.*² revealed clearly multiple branches of excitations in quantum-dot arrays. As we have shown above, both multiple branches and anticrossings can be explained qualitatively by our theory. However, a detailed quantitative comparison to the results in Ref. 2 has not been possible. This is because the experiments were performed for $n_0=25-210$, while calculations for large n_0 values require very long computing time, and we have only performed calculations for up to $n_0=6$ at finite B . Further experimental results for smaller values of n_0 would be of considerable interest. According to our theory, anticrossings can occur only when $n_0 > 2$. This prediction can be tested experimentally.

D. Effect of electron transfer between energy levels

As shown in Fig. 1, quantum confinement causes level crossings in the single-particle energy spectrum. For a fixed number of electrons, level crossings can cause electrons to be transferred between energy levels as the magnetic field changes. Let us consider the zero temperature case. If there are five or six electrons per dot, at $B=0$ the $(0,1)$ level is occupied and the $(0,-2)$ level is empty. As B increases the two levels approach each other and cross at $B=B_c$, as Fig. 1 indicates. At the crossing point, electrons are transferred from the $(0,1)$ level into the $(0,-2)$ level, and the angular quantum number m for the top occupied level changes abruptly from $m=1$ to $m=-2$. The sudden change in the quantum number m affects the matrix elements for Coulomb interaction and manifests itself in the collective spectrum. In Fig. 4(a) the solid curves in the collective excitation spectrum at zero temperature show discontinuities at $B=B_c$. Note that only level crossings at the Fermi level cause charge transfer and thus anomalies in collective spectra. The discontinuities are artifacts of zero temperature for which the charge transfer occurs suddenly at the point $B=B_c$. At finite temperatures, charge transfer becomes a gradual process. The dashed lines in Fig. 4 are for $T=2$ K. The discontinuities are smoothed out. This is because near $B=B_c$, the energies of the two energy levels can be arbitrarily close. If the energies measured from the chemical potential (Fermi level) are comparable to the thermal energy $k_B T$, both levels become partially occupied with significant occupancy factors. As B increases across B_c , the occupancy in the $(0,1)$ level decreases continuously, and that in the $(0,-2)$ level increases continuously. The

width of the region in which both levels have significant occupancy determines the experimental difficulty to observe this electron transfer effect. The lower the temperature is, the narrower this region is and the easier to observe the effect. This effect should be easier to identify in derivative of energy against B plots as shown in Fig. 4(b). Peaks or valleys occur at B_c in such plots.

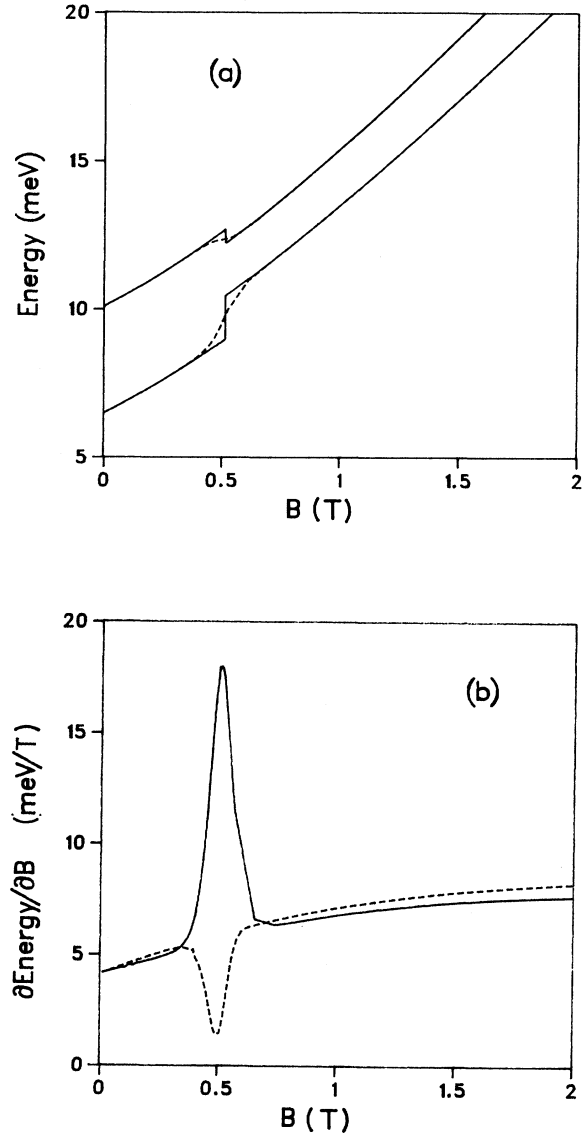


FIG. 4. (a) Two positive B dispersion branches for the $n_0=6$ case. The solid lines are for zero temperature, and the dashed lines are for $T=2$ K. Other parameters are the same as in Fig. 2. Singularities occurring at 0.51 T are caused by electron transfer between energy levels. (b) Derivatives of the dashed lines in (a). The solid (dashed) curve corresponds to the lower (upper) dashed curve in (a).

E. Coulomb interaction between dots versus inside dots

Energies of collective excitations are shifted from single-particle excitation energies. The shift is caused by Coulomb interaction between electrons, which exists between electrons in different quantum dots as well as those in the same dot. We wish to point out that our ansatz takes into account both interdot and intradot Coulomb interactions. This can be shown explicitly by the following. The Coulomb interaction between electrons is treated in Eq. (2.4) by the matrix element $\langle a | V | a' \rangle$, where V is the Coulomb potential. After substituting $|a\rangle, |a'\rangle$ by tight-binding states of the form (2.1), we get two kinds of terms: (a) Terms involving basis states located on different dots, which take care of the interdot Coulomb interaction; (b) terms involving basis states located on the same dot, which take care of the intradot Coulomb interaction.

Coulomb coupling between dots is expected to decrease as the separation between dots becomes larger. One might think that the depolarization shift is predominantly due to the interaction of electrons in the same dot, because of the shorter distances between electrons in the same dot thus stronger interaction compared to electrons in different dots. However, a closer examination of this naive view shows that one cannot arrive at a clear-cut conclusion. We must remember that the Coulomb force is long range, and an electron in a given dot interacts with far more electrons in other dots than the limited number of electrons in the same dot. In other words, in the contribution to collective excitations, the Coulomb interaction between dots, although weaker, has a much larger weighting factor. Therefore from simple arguments it is difficult to decide which interaction is more important for collective excitations, and the question can only be answered by detailed calculations.

Figure 5 shows the dependence of energy shift on d , the lattice constant of a square lattice of quantum dots. The energy in excess of $\hbar\omega_0 = 6$ meV is due to depolarization shift. The lower curve is for one electron per dot, thus by definition the shift is purely due to Coulomb coupling between dots. All FIR experiments performed so far on quantum-dot arrays have d less than 1000 nm. Figure 5 indicates that the energy shift due to Coulomb coupling between dots should be significant for $d < 1000$ nm.

While it is expected that in the $d \rightarrow \infty$ limit, the energy shift in the $n_0 = 1$ case should approach zero, it is astonishing to see in Fig. 5 that for $n_0 = 4$ the energy shift also approaches zero in this limit. In fact, Eq. (3.9) implies that for $q = 0$, the energy shift approaches zero in the $d \rightarrow \infty$ limit for any n_0 . Mathematically this is because the Bessel function in Eq. (3.9), $J_{m-m'}(\rho q (\hbar/m^* \Omega)^{1/2})$, is zero if the argument is zero and $m \neq m'$. ($m = m'$ is not allowed by the selection rules.) In the $d \rightarrow \infty$ limit the lattice constant for the reciprocal lattice $2\pi/d \rightarrow 0$. Thus for $q = 0$ the Bessel function is always evaluated at zero, giving no energy shift.

Since the self-consistent-field formalism and the tight-binding ansatz we used are not exact methods, this is not an exact result. The physical implication of this result is

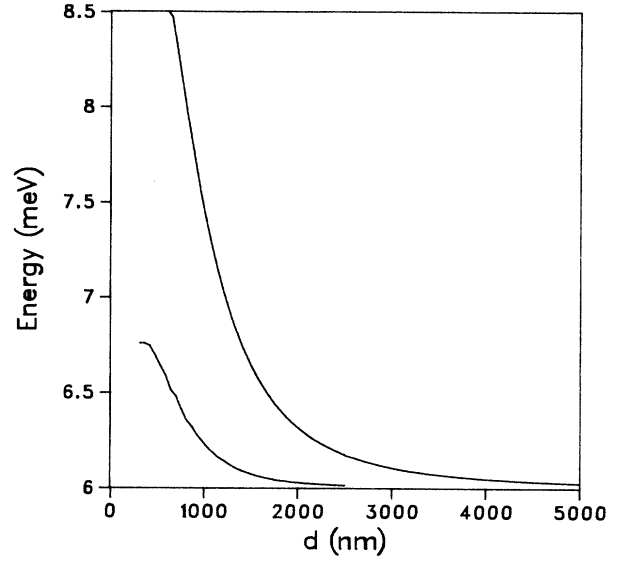


FIG. 5. Collective excitation energy as a function of distance. d is the center to center distance between neighboring dots in a square lattice array. Lower curve: $n_0 = 1$; upper curve: $n_0 = 4$. $B = 0$ T. Other parameters are the same as in Fig. 2. Since $\hbar\omega_0 = 6$ meV, the energy in excess of 6 meV is the depolarization shift.

that for $q = 0$, the intradot Coulomb interaction causes negligible energy shift. In fact, for $q = 0$ it can be proven exactly that for a single quantum dot with a parabolic external confining potential, the interaction between electrons in the dot does not cause any energy shift in optical excitations.¹⁹ Our result is consistent with this so-called “generalized Kohn’s theorem.”

For $q \neq 0$, the intradot Coulomb interaction does contribute to the energy shift in our calculations. In Sec. IV we will show that the energy dispersion of collective energy is generally small, typically less than 0.1 meV. Thus in the $q \neq 0$ case for $d < 1000$ nm the energy shift is mainly due to the Coulomb coupling between dots.

The above results show that the intradot Coulomb interaction is relatively unimportant for optical excitations. We are not the first to arrive at this conclusion. The generalized Kohn’s theorem provided the first convincing evidence for this conclusion. This highlights the importance of interdot coupling in quantum-dot arrays.

F. Saturation behavior

Figure 6 shows the dependence of collective energy on the number of electrons per dot. The horizontal lines show single-particle excitation energies in Eq. (3.7). Up to $n_0 = 3$, the collective energy increases by significant amounts, but beyond that point the energy increases very slowly. This saturation behavior is a unique property of quantum-dot systems. It can be most easily understood by considering the $B = 0$, zero-temperature case for a sys-

tem with no degeneracy other than the spin degeneracy. In this case selection rules for dipole transitions require that excitations occur only between neighboring energy levels. Suppose the system has at least four levels. For $n_0=1$ or 2, electrons can be excited from the populated first level to the empty second level. For $n_0=3$, the second level is only half filled, electrons in the first level can still be excited to the second level. In addition the electron in the second level can be excited to the third level. Thus up to $n_0=3$, all electrons can be activated, and the collective excitation energy in a quantum-dot array increases. However, if $n_0=4$, electrons in the first level can no longer be excited, because the second level is full, and excitations to higher levels from the first level are forbidden by the selection rules. Only electrons in the second level contribute to collective excitations. In this system the number of electrons participating in collective excitations cannot exceed three per dot. As n_0 increases and more levels are filled, only electrons in one or two levels at or near the Fermi level can be activated; electrons in lower-energy levels are inactive. This causes saturation in the collective spectrum. For degenerate states as in the parabolic confining potential model, each state in a degenerate multiplet has its unique symmetry properties, and selection rules only allow certain symmetry states to accept excitations from a given lower level. The number of electrons that can participate in excitations is still limited. A finite magnetic field makes the situation more complicated, but as shown in Fig. 6 the saturation behavior remains.

The saturation behavior in quantum-dot systems is a contrast to quantum-wire systems. In quantum wires, all energy subbands below the Fermi level are only *partially*

occupied, a result of the free motion in the direction of a wire. Excitations from all populated subbands are always allowed, making all subbands contribute to collective excitations. The result is that the collective energy increases with electron density without saturation in quantum-wire systems.^{11,15} In Ref. 4 the authors reported FIR data on quantum-dot arrays in the range of $n_0=3-20$. The FIR resonance energy was found to be insensitive to n_0 within experimental error. With no theoretical results for the n_0 dependence available at that time, the authors drew the conclusion that in their system collective modes are suppressed, based solely on the insensitivity of the excitation energy to n_0 . Now it is clear that this conclusion was unwarranted, because the insensitivity to n_0 in the experimental data is entirely consistent with the FIR resonances being collective excitations.²¹ Further independent measurements of the single-particle excitation energy in the same sample should give an energy lower than the FIR resonance energy.

IV. NONLOCALITY

A standard approximation in theories of collective excitations is the local approximation, which corresponds to the long-wavelength limit $q \rightarrow 0$. Translating into real space, this approximation is equivalent to neglecting non-local effects, which can only be included by considering higher-order terms in q . For many systems the local approximation works well and is very useful. However, for

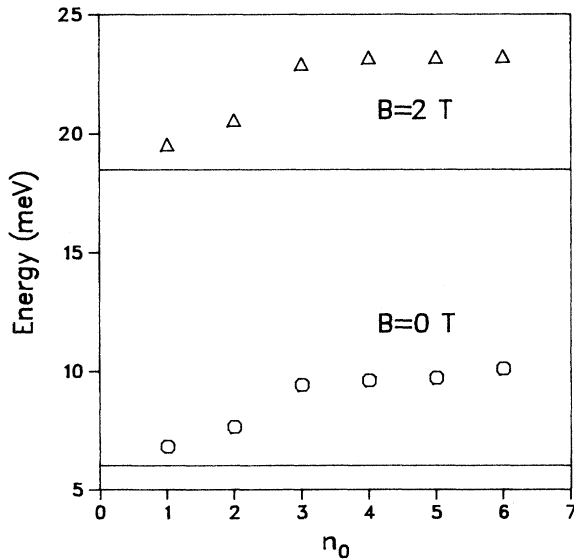


FIG. 6. Collective excitation energy as a function of n_0 . $B=0$ T for the lower curve, and 2 T for the upper curve. Other parameters are the same as in Fig. 2. The solid lines indicate the single-particle energies in Eq. (3.7).

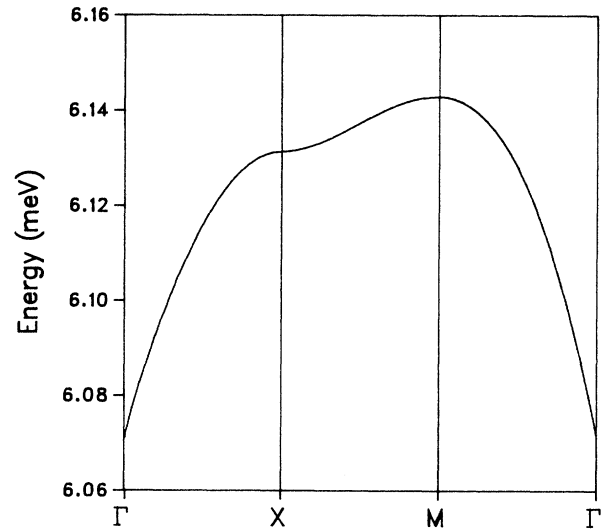


FIG. 7. Wave-vector dispersion of a negative B dispersion collective mode for $n_0=4$, $B=2$ T. Other parameters are the same as in Fig. 2. Γ , X , and M represent, respectively, the following points in k space: $(0,0)$, $(\pi/d,0)$, and $(\pi/d,\pi/d)$.

the problem under study here this approximation is inappropriate. For example, this approximation fails to produce a nonzero depolarization shift at $q=0$ for any confining potential, while a more precise nonlocal theory predicts significant depolarization shifts.

Our theory is a nonlocal theory, valid for any wave vector. In fact, for dispersionless quantum-dot systems, our theory is exact as far as nonlocality is concerned. This is achieved by carrying out exactly the summation over the reciprocal lattice vector \mathbf{G} to infinite order in Eqs. (2.10)–(2.16). This nonlocal feature of our theory ensures that the Coulomb coupling between dots is treated properly.

An interesting result of our theory is that a system with a dispersionless single-particle energy spectrum can have a dispersive collective energy spectrum. An example has been presented in Fig. 1 of Ref. 3 for the zero magnetic field case. Here in Fig. 7 we show an example for the finite magnetic field case. The dispersion will increase if the background dielectric constant is reduced. However, the dispersion is generally a small effect, which makes experimental measurements of the dispersion difficult.

For symmetric confining potentials and $q=0$, the dipole excitations allowed by the selection rules are decoupled from the “ $2\omega_c$ ” modes,²² which are forbidden by the dipole selection rules. For $q \neq 0$, the dipole excitations in principle couple to the $2\omega_c$ modes. However, this coupling is unlikely to be observable in quantum-dot systems.

One reason is the generally small wave-vector dispersions for all modes, which imply the coupling is expected to be very small. Another reason is that because optical (FIR) wavelengths are much larger than quantum-dot sizes, such probes are not suitable for creating excitations forbidden by the dipole selection rules.

V. OSCILLATOR STRENGTHS

The oscillator strengths for circularly polarized optical transitions from state $|a\rangle$ to state $|a'\rangle$ are given by

$$f_{\pm}(a \rightarrow a') = \frac{2m^*(E_{a'} - E_a)}{\hbar^2} |\langle a' | (x \pm iy) | a \rangle|^2. \quad (5.1)$$

For dispersionless quantum-dot arrays, overlap integrals vanish, and (5.1) equals that for a single quantum dot,

$$f_{\pm}(nm \rightarrow n'm') = \frac{2m^*(E_{n'm'} - E_{nm})}{\hbar^2} \times |\langle n'm' | (x \pm iy) | nm \rangle|^2. \quad (5.2)$$

Using (3.5) and (3.6), we find

$$f_{\pm}(nm \rightarrow n'm') = 2 \left[1 \pm \frac{\hbar\omega_c}{2\hbar\Omega} \right] \delta_{m', m \pm 1} \times \begin{cases} \left[n + m + \frac{1 \pm \text{sgn}(m)}{2} \right] \delta_{n', n} + \left[n + \frac{1 \mp \text{sgn}(m)}{2} \right] \delta_{n', n \mp \text{sgn}(m)}, & m \neq 0, \\ (n+1)\delta_{n', n} + n\delta_{n', n-1}, & m = 0. \end{cases} \quad (5.3)$$

The factor $(1 \pm \hbar\omega_c/2\hbar\Omega)$ becomes 1 if $B=0$, and in the $B \rightarrow \infty$ limit it becomes 2 for the + sign, 0 for the – sign. The oscillator strengths for positive B dispersion branches increase as B increases, while those for negative B dispersion branches decrease. This is consistent with the experiments in Ref. 2.

The oscillator strengths defined in (5.1) are for isolated, or decoupled single-particle type optical transitions. In FIR experiments different transitions coexist and they are in general coupled. The coupling can redistribute oscillator strengths among various modes. In multiwire superlattices¹¹ with parabolic confinement, it was found that the coupling of N dipole modes leads to one strong mode with a large energy shift, and $N-1$ weak modes with very small energy shifts. This drastic coupling effect is related to the fact that matrix elements of the operator $e^{i\mathbf{q}\cdot\mathbf{r}}$ do not vary too much.¹¹ For quantum-dot systems with parabolic confinement, the effect of coupling does

not seem to be as drastic. As Fig. 3(b) shows, for example, the two positive B dispersion branches both have significant energy shifts from the single-particle excitation energy. This reflects the stronger dependence of the matrix elements on quantum indices in quantum-dot systems.

The selection rules or Eq. (5.3) imply that single-particle excitations in the system are either left or right circularly polarized. If one uses circularly polarized lights as probes, one can selectively excite modes with a particular circular polarization. However, collective modes labeled by $\Delta m = 1$ and -1 can be coupled. Therefore the use of circularly polarized lights will predominantly detect, for example, the $\Delta m = 1$ modes, but signals from the “forbidden” $\Delta m = -1$ modes may also appear in the spectra. The strengths of the “forbidden” modes provide information on the coupling strengths between the $\Delta m = 1$ and -1 modes.

VI. CONCLUDING REMARKS

The study of quantum-dot systems is a developing field. The understanding of FIR experiments on quantum-dot systems has been very limited. It is not our intention to explain every possible phenomenon in this paper, although we have tried to discuss the topics that have already attracted the attention of workers in this field.

So far only the FIR transmission-absorption method has been used to study collective excitations in quantum dots. Its drawback is that it cannot directly measure single-particle energies to offer comparisons to collective energies. It will be interesting to try other optical methods, such as Raman scattering, which can directly measure single-particle energies.

According to our explanation, anticrossings occur in the excitation spectrum of quantum-dot arrays if the confining potential of a dot deviates from the ideal parabolic shape. The breaking of azimuthal symmetry or deviations from the parabolic shape by artificial means should enhance the anticrossing behavior. This suggests that samples with rectangular-shaped cap layers instead of square-shaped cap layers should exhibit stronger anticrossing behavior. No experiments on samples with rectangular-shaped cap layers have been performed. Such experiments will be very interesting. It is likely that the confining potential in the sample studied in Ref. 2 deviates significantly from the parabolic model.

We also propose the following experiments to be done in future research: experiments with circularly polarized lights; experiments on samples with small n_0 ; independent measurements of single-particle energy spacings in comparison with FIR resonance energies; and the temperature dependence of multiple branches and anticrossings. Several effects which should or might be observable are yet to be observed. They include the following: the disappearance or reduction in signal strengths of some branches when circularly polarized lights are used; the disappearance of anticrossing when n_0 is changed from $n_0 > 2$ to $n_0 \leq 2$; the lifting of degeneracy at $B=0$; the effect of electron transfer between energy levels; and the dispersion in the collective energy spectrum for a dispersionless single-particle energy spectrum.

Our discussions have been limited to lower magnetic fields, where spin splitting is negligible. At higher magnetic fields we can expect large spin splitting which can affect the collective spectrum. So far no experiments

have reported effects of spin splitting. We leave this topic to future research.

Excitonic effects are neglected in the present theory. Their importance in quantum-dot arrays remains to be clarified. One may argue that such effects should be small in quantum-dot arrays because they represent local field corrections, while the depolarization shift in quantum-dot arrays is mainly due to interdot coupling.

The parabolic confinement model is very useful, but it has its limitations. For any finite-size quantum dot this model must break down near the edges. It should be the best for lower-energy states whose wave functions are more squeezed toward the central region. Thus it should work at its best when n_0 is small, such that excitations do not involve states too high in energy. The symmetric parabolic confinement model does not allow us to study anticrossing effects in the single-particle energy spectrum, which can happen for confining potentials without circular symmetry.²³

In conclusion, we have developed a nonlocal quantum theory of collective excitations in quantum-dot arrays. We hope this theory will encourage experimentalists to carry out additional experiments, which will in turn raise more interesting questions for theorists to answer.

Note added in proof. There has been some confusion over the interpretation of the confining potential used in the self-consistent-field formalism. Some authors interpret it as the external confining potential, others interpret it as the screened self-consistent confining potential. We note that, from the diagrammatic Green-function approach,²⁴ it is clear that within the random-phase approximation the correct interpretation of the confining potential should be the external confining potential. To see this, the Hamiltonian of the system is written as $H = H_0 + V$, where H_0 is the free-electron part plus the external confining potential, V is the electron-electron interaction part. The unperturbed polarization Π in (2.11) is derived from products of unperturbed Green functions corresponding to H_0 . Thus the eigenstates used in Π should be those corresponding to H_0 , and the confining potential should be the external confining potential.

ACKNOWLEDGMENTS

W.Q. would like to thank Hang Shi for useful conversations.

¹For an overview, refer to Phys. Today **43** (2) (1990), where several interesting articles can be found.

²T. Demel, D. Heitmann, P. Grambow, and K. Ploog, Phys. Rev. Lett. **64**, 788 (1990).

³W. Que and G. Kirczenow, Phys. Rev. B **38**, 3614 (1988).

⁴Ch. Sikorski and U. Merkt, Phys. Rev. Lett. **62**, 2164 (1989).

⁵J. Alsmeyer, E. Batke, and J. P. Kotthaus, Phys. Rev. B **41**, 1699 (1990).

⁶A. Lorke, J. P. Kotthaus, and K. Ploog, Phys. Rev. Lett. **64**, 2559 (1990).

⁷H. Böttger and V. V. Bryksin, *Hopping Conduction in Solids* (Akademie-Verlag, Berlin, 1985).

⁸H. Ehrenreich and M. H. Cohen, Phys. Rev. **115**, 786 (1959).

⁹W. Que and G. Kirczenow, Phys. Rev. B **36**, 6596 (1987).

¹⁰S. Das Sarma and J. J. Quinn, Phys. Rev. B **25**, 7603 (1982).

¹¹W. Que and G. Kirczenow, Phys. Rev. B **39**, 5998 (1989); **37**, 7153 (1988).

¹²Q. Li and S. Das Sarma, Phys. Rev. B **41**, 10 268 (1990); and (unpublished).

¹³A. Kumar, S. E. Laux, and F. Stern, Phys. Rev. B **42**, 5166 (1990).

¹⁴V. Fock, Z. Phys. **47**, 446 (1928); C. G. Darwin, Proc. Cambridge Philos. Soc. **27**, 86 (1930).

¹⁵W. Hansen *et al.*, Phys. Rev. Lett. **58**, 2586 (1987); F. Brin-

- kop, W. Hansen, J. P. Kotthaus, and K. Ploog, *Phys. Rev. B* **37**, 6547 (1988).
- ¹⁶M. A. Reed *et al.*, *Phys. Rev. Lett.* **60**, 535 (1988).
- ¹⁷A. Tselis and J. J. Quinn, *Phys. Rev. B* **29**, 3318 (1984); P. Hawrylak, J. W. Wu, and J. J. Quinn, *ibid.* **32**, 5169 (1985).
- ¹⁸W. Que, *Phys. Rev. B* **43**, 7127 (1991).
- ¹⁹P. A. Maksym and T. Chakraborty, *Phys. Rev. Lett.* **65**, 108 (1990); F. M. Peeters, *Phys. Rev. B* **42**, 1486 (1990); L. Brey, N. F. Johnson, and B. I. Halperin, *ibid.* **40**, 10 647 (1989).
- ²⁰V. Gudmundson and R. R. Gerhardt, Proceedings of the International Conference on High Magnetic Fields in Semiconductor Physics, Würzburg, 1990 (unpublished).
- ²¹W. Que, *Phys. Rev. Lett.* **64**, 3100 (1990).
- ²²E. Batke, D. Heitmann, J. P. Kotthaus, and K. Ploog, *Phys. Rev. Lett.* **54**, 2367 (1985).
- ²³M. Robnik, *J. Phys. A* **19**, 3619 (1986).
- ²⁴See, for example, G. D. Mahan, *Many-Particle Physics* (Plenum, New York, 1981), p. 426.